

Cite this: *Dalton Trans.*, 2023, **52**, 1501Received 29th September 2022,  
Accepted 21st December 2022

DOI: 10.1039/d2dt03161b

rsc.li/dalton

## Ferrocene-triazole conjugates: do we know why they are biologically active?

Mariola Koszytkowska-Stawińska\* and Włodzimierz Buchowicz \*

The bioorganometallic chemistry of ferrocene has been gaining significance in recent years. This review presents ferrocene-triazole conjugates displaying significant biological properties. The conjugates have been synthesized *via* azide–alkyne cycloaddition reactions. The data are summarized according to the type of activity (anticancer, antibacterial and/or antifungal, antiprotozoal, and other effects). The results of studies concerning the understanding of the role of the ferrocene core in their biological activity are highlighted. While generally the mode of action of these organometallic species remains unclear, the importance of redox properties of ferrocene has been postulated in several cases.

### 1 Introduction

Ferrocene was serendipitously discovered in a laboratory 71 years ago.<sup>1,2</sup> This air-stable, sparingly water-soluble<sup>3,4</sup> organometallic compound is usually considered as exhibiting low toxicity.<sup>5,6</sup> While ferrocene derivatives have not been found in nature, their bioorganometallic chemistry commenced with the discovery of anticancer properties of ferrocene polyamides<sup>7</sup> and cationic ferrocenium species.<sup>8,9</sup> Ferroquine<sup>10</sup> and ferrocifens<sup>11–14</sup> are the most widely known ferrocene derivatives displaying significant biological activity.

Ferrocene-triazole hybrids have attracted considerable scientific attention since the ferrocene-benzotriazole conjugate was found to possess antitumor activity *in vivo*.<sup>5,6,15</sup> Several reasons for interest in 1*H*-1,2,3-triazoles might be emphasized.

From the preparative point of view, the 1*H*-1,2,3-triazole platform can be easily prepared *via* the azide–alkyne cycloaddition of two readily accessible substrates.<sup>16</sup> Owing to the specific electron density, the 1*H*-1,2,3-triazole ring might serve as an isostere of an amide or ester bond, or of a heterocyclic moiety.<sup>17</sup> 1*H*-1,2,3-Triazoles can also be considered as isosteres of a carboxylic acid moiety or rigid analogues of olefins. Moreover, by H-bonding or  $\pi$ – $\pi$  stacking interactions, the 1*H*-1,2,3-triazole moiety might serve as a centre of interactions with a biological target.<sup>17,18</sup> There are also numerous examples of 1*H*-1,2,3-triazoles with biological properties,<sup>19–21</sup> including commercial or investigational drugs.<sup>22</sup> The 1*H*-1,2,3-triazoles are not metabolized.<sup>23</sup> Thus, they can be considered as risk-free building blocks in target drug candidates.

The ferrocene-1*H*-1,2,3-triazole conjugates discussed in this review have been synthesized using copper- or ruthenium-catalysed azide–alkyne cycloaddition (click-chemistry), as shown in Scheme 1. Two general approaches have been used: with a ferrocene-bearing azide (method 1), or alternatively with a ferrocene-bearing alkyne (method 2). In both cases, the azide/alkyne group has been linked directly to ferrocene (methods 1a, 2a), or separated from ferrocene with a linker of variable length and structure. These synthetic routes resulted in a considerable variety of conjugates with diverse structures and properties.

In this review the literature since 2012 has been covered. Only sparse examples of biologically active ferrocene-1*H*-1,2,3-triazole conjugates were collected in the previous review on ferrocene-derived triazoles.<sup>24</sup> Recently, more general accounts of the biological properties of ferrocene-organic hybrids have also been found.<sup>25–30</sup> Nonetheless, the concept of ferrocene-1*H*-1,2,3-triazole conjugates was not discussed in detail in these publications.

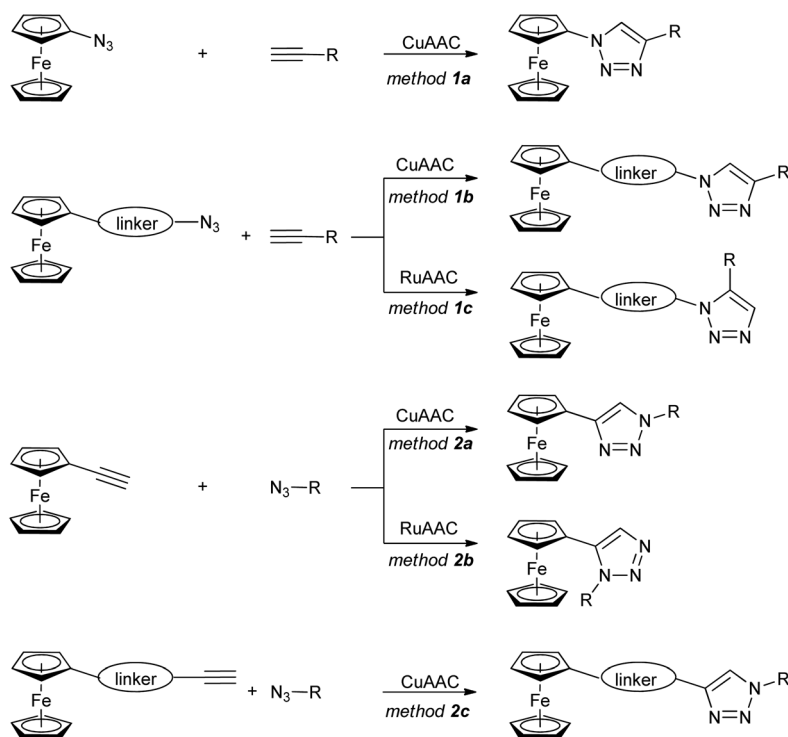
The biologically active conjugates are reviewed in Tables 1–4 according to the type of their activity (anticancer, antibacterial and/or antifungal, antiprotozoal, and other effects). The synthetic route is also shown in the first column of each table. The results of studies dealing with the mechanism of action of the examined compounds (including the biological role of the ferrocene moiety) are presented in detail.

### 2 Conjugates with anticancer activity

By far the largest number of compounds was tested for anticancer activity (Table 1). In a majority of reports covered in this section, the following structural features were noted: (a) a non-hydrolysing connection (*i.e.* other than ester or amide)

Faculty of Chemistry, Chair of Organic Chemistry, Warsaw University of Technology, Noakowskiego 3, 00-664 Warsaw, Poland. E-mail: włodzimierz.buchowicz@pw.edu.pl





**Scheme 1** General synthetic approaches for ferrocene-1H-1,2,3-triazole conjugates of biological interest. CuAAC – copper catalysed azide–alkyne cycloaddition. RuAAC – ruthenium catalysed azide–alkyne cycloaddition.

between ferrocene and the organic part of the molecule (for exceptions, see entries 1.15, 1.16, 1.26 and 1.29), (b) mono-substitution of ferrocene (for exceptions, see entries 1.11 and 1.18), or (c) the 1,4-disubstitution pattern of the 1H-1,2,3-triazole ring (for a few conjugates with the 1,5-disubstitution pattern, see entry 1.18; for an unusual conjugate with a 1,4,5-trisubstituted-1H-1,2,3-triazole ring, see entry 1.20). Post click-synthesized conjugates were surprisingly rare (entries 1.20 and 1.30). Interestingly, studies concerning conjugates bearing structural motifs of natural origin were very ubiquitous (entries 1.1 and 1.20 – polyhydroxy phenols; entries 1.11, 1.12, 1.13 and 1.14 – nucleobases; entry 1.18 – alkaloids; or entries 1.16, 1.26, 1.27 and 1.28 – carbohydrates). It is worth pointing out entry 1.11 with an *ansa*[4]-ferrocene (ferrocenophane) conjugate that appeared more active than its unbridged counterpart (entry 1.12).

The reported values of  $\text{IC}_{50}$  were in the micromolar range with the highest anticancer activity determined for the amino-quinoline conjugate ( $\text{IC}_{50}$  0.37  $\mu\text{M}$ , entry 1.19). We would like to emphasize that the activities of several conjugates collected in Table 1 are of the same order of magnitude as those of ferrocifen type derivatives.<sup>11–14</sup>

In a majority of studies, the mechanism of the observed biological effect was not investigated, that is understanding of the role of the ferrocene moiety is generally lacking. The notable exceptions include the report by Maračić *et al.*<sup>32</sup> on quinoline–ferrocene conjugates (entries 1.2, 1.6 and 1.7) where low antioxidant activity of the most active compounds was

determined (entries 1.2 and 1.7). Furthermore, the cell cycle and intracellular generation of ROS (reactive oxygen species) were studied revealing accumulation in the G0/G1 phase for the two compounds. However, only one compound (entry 1.2) was found to significantly increase the ROS generation in *Raji* cells.<sup>32</sup> The physicochemical properties, such as solubility and metabolic stability in liver microsomes, of purine- and purine isostere-tagged ferrocenes were thoroughly investigated (entries 1.3, 1.4, 1.5, 1.8, 1.9, 1.21).<sup>33</sup> However, conclusions on the mode of action of these cytotoxic conjugates were not given.

Djaković *et al.* studied mono- and bis-ferrocene uracil conjugates (entries 1.13 and 1.14, respectively).<sup>35</sup> Selected bis-ferrocene derivatives (entry 1.14) were further evaluated for intracellular ROS accumulation, mitochondrial membrane dysfunction activity, and apoptosis induction. The results suggested that the activity might be due to the disruption of the mitochondrial membrane potential and the ability to induce apoptosis in cancer cells.

Detailed studies on the mechanism of cytotoxicity of ferrocenyl dipyridylamines, Zn(II) or Cu(II) complexes (entry 1.17), revealed an increase in the number of cells in the S and G2/M phase of the cell cycle. The authors concluded that the Cu(II) complex did not interfere with DNA synthesis but induced replication stress in the cancer cells, probably as a result of complex–protein interactions.<sup>38</sup>

A series of 1H-1,2,3-triazole-tethered hybrids 1–7 bearing a cinchona alkaloid-ferrocene couple was designed and prepared



**Table 1** Ferrocene-triazole conjugates with anticancer activity<sup>a</sup>

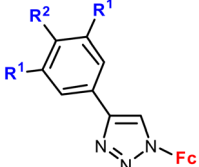
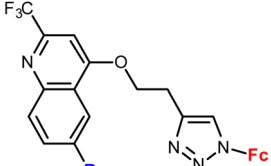
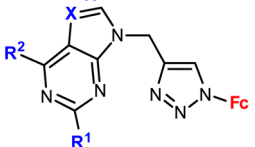
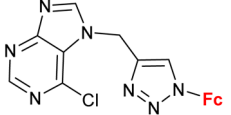
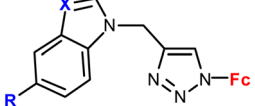
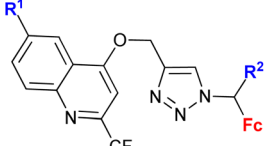
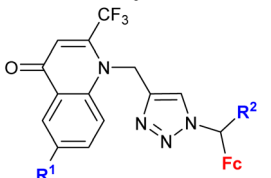
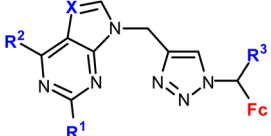
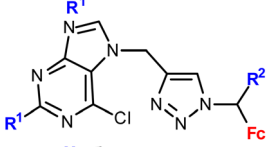
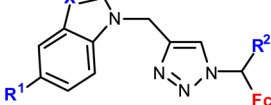
Entry/synthesis <sup>b</sup> structure and number of compounds examined	IC <sub>50</sub> or EC <sub>50</sub> [μM] (cell line) number of cancer cell lines studied	Ref.	
<b>1.1/1a</b> 	R <sup>1</sup> = H or OH R <sup>2</sup> = H or OH (2 compounds)	48.9 ( <i>HCC38</i> ) R <sup>1</sup> = H, R <sup>2</sup> = OH 2 cell lines	31
<b>1.2/1a<sup>c</sup></b> 	R = H, Me, Cl, Ph (4 compounds)	7.9 ± 0.6 ( <i>Raji</i> ) R = Cl 4 cell lines	32
<b>1.3/1a</b> 	R <sup>1</sup> = H, NH <sub>2</sub> R <sup>2</sup> = Cl, NH <sub>2</sub> X = CH or N (4 compounds)	9.07 ± 1.21 ( <i>SW620</i> ) R <sup>1</sup> = H, R <sup>2</sup> = Cl, X = CH 4 cell lines	33
<b>1.4/1a</b> 		45.47 ± 4.52 ( <i>SW620</i> ) 4 cell lines	33
<b>1.5/1a</b> 	R = H or I X = CH or N (3 compounds)	71.79 ± 3.44 ( <i>HepG2</i> ) R = I, X = CH 4 cell lines	33
<b>1.6/1b<sup>c</sup></b> 	R <sup>1</sup> = H, Me, Cl, Ph R <sup>2</sup> = H or Me (8 compounds)	95.89 ± 2.4 ( <i>K562</i> ) R <sup>1</sup> , R <sup>2</sup> = Me 4 cell lines	32
<b>1.7/1b<sup>c</sup></b> 	R <sup>1</sup> = H, Me, Cl, Ph R <sup>2</sup> = H or Me (4 compounds)	7.73 ± 2.4 ( <i>K562</i> ) R <sup>1</sup> , R <sup>2</sup> = H 4 cell lines	32
<b>1.8/1b</b> 	R <sup>1</sup> = H, Cl, NH <sub>2</sub> R <sup>2</sup> = H, Cl, NH <sub>2</sub> X = CH, N R <sup>3</sup> = H or Me (8 compounds)	14.38 ± 3.02 ( <i>SW620</i> ) R <sup>1</sup> , R <sup>3</sup> = H, R <sup>2</sup> = Cl, X = CH 4 cell lines	33
<b>1.9/1b</b> 	R <sup>1</sup> = H or NH <sub>2</sub> R <sup>2</sup> = H or Me (3 compounds)	15.50 ± 3.24 ( <i>SW620</i> ) R <sup>1</sup> = H, R <sup>2</sup> = Me 4 cell lines	33
<b>1.10/1b</b> 	R <sup>1</sup> = H or I R <sup>2</sup> = H or Me X = CH or N (6 compounds)	53.55 ± 5.05 ( <i>HepG2</i> ) R <sup>1</sup> , R <sup>2</sup> = H, X = CH 4 cell lines	33



Table 1 (Contd.)

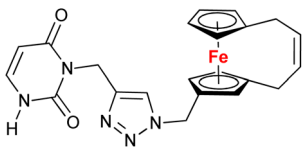
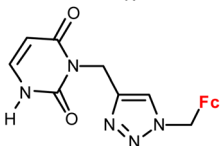
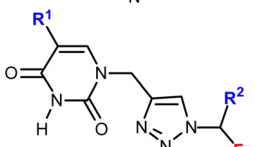
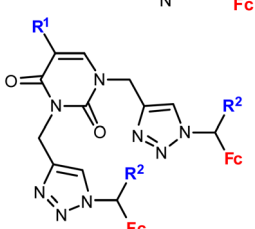
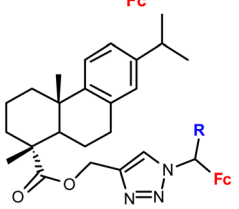
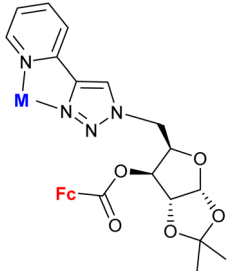
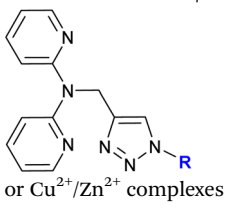
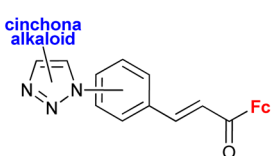
Entry/synthesis <sup>b</sup> structure and number of compounds examined	IC <sub>50</sub> or EC <sub>50</sub> [μM] (cell line) number of cancer cell lines studied	Ref.	
1.11/1b 	10.9 ± 1.7 (A549) 3 cell lines	34	
1.12/1b 	28.5 ± 2.2 (A549) 3 cell lines	34	
1.13/1b <sup>c</sup> 	R <sup>1</sup> = H, Me, Cl, Br, I R <sup>2</sup> = H or Me (10 compounds)	11.9 ± 6.4 (K562) R <sup>1</sup> = I, R <sup>2</sup> = H 4 cell lines	35
1.14/1b <sup>c</sup> 	R <sup>1</sup> = H, Me, Cl, Br, I R <sup>2</sup> = H or Me (10 compounds)	2.0 ± 0.8 (Raji) R <sup>1</sup> = H, R <sup>2</sup> = Me 4 cell lines	35
1.15/1b 	R = H or Me (2 compounds)	46.17 ± 9.65 (RD) 3 cell lines	36
1.16/1b 	M = PdCl <sub>2</sub> or ∅ (2 compounds)	5.73 ± 0.03 (A549) M = ∅ 4 cell lines	37
1.17/1a or 1b <sup>c</sup> 	R = Fc, FeCH <sub>2</sub> or FeCH(CH <sub>3</sub> ) (3 ligands, 6 complexes)	14.0 ± 1.4 (HeLa) R = FeCH(CH <sub>3</sub> ), Cu <sup>2+</sup> complex 5 cell lines	38
1.18/1b or 1c <sup>c</sup> 	16 compounds for details see Scheme 2	0.7 ± 0.1 (HepG2) 5 cell lines	39 and 40

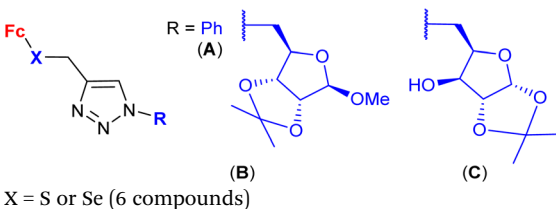
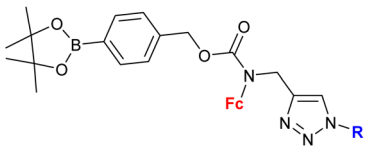
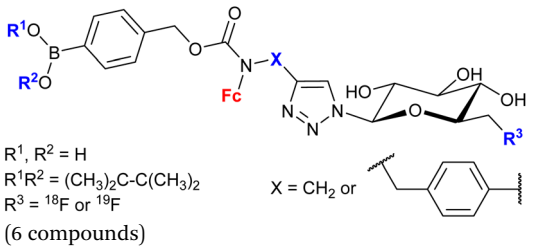
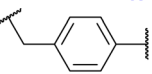
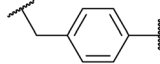
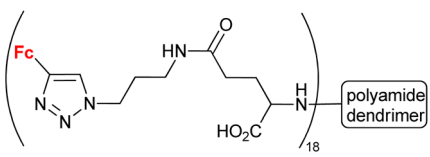


Table 1 (Contd.)

Entry/synthesis <sup>b</sup> structure and number of compounds examined	IC <sub>50</sub> or EC <sub>50</sub> [μM] (cell line) number of cancer cell lines studied	Ref.	
1.19/1b 	0.37 ( <i>HeLa</i> ) $m = 2, n = 5$ 1 cell line	41	
1.20/2a 	$R^1 = \text{H or OH}$ $R^2 = \text{H or OH}$ $R^3 = \text{H or C}_6\text{H}_4\text{-OH-4}^d$ (5 compounds)	15.3 ( <i>HCC38</i> ) $R^1 = \text{H}, R^2 = \text{OH}, R^3 = \text{H}$ 2 cell lines	31
1.21/2a 	$R = \text{Cl, pyrrolidin-1-yl, morpholin-1-yl}$ $X = \text{CH or N}$ (6 compounds)	45.78 ± 9.11 ( <i>CFPAC-1</i> ) $R = \text{morpholin-1-yl}, X = \text{CH}$ 4 cell lines	33
1.22/2a 	$R = \text{Me, Et, Ph}$ (3 compounds)	48.71 ± 3.55 ( <i>MS</i> ) $R = \text{Me}$ 3 cell lines	42
1.23/2a <sup>e</sup> 	Sugar = protected: (A) 5-deoxy-β-D-ribofuranos-5-yl, (B) 5-deoxy-α-D-xylofuranos-5-yl, (C) 6-deoxy-α-D-glucopyranos-6-yl, (D) 6-deoxy-α-D-galactopyranos-6-yl	5.3 ( <i>MDA-MBA-231</i> ) $R = \text{A}$ 5 cell lines	43
1.24/2a or 2b 	$R^1 = \text{Fc or FcCH}_2^f$ $R^2 = \text{CH}_2\text{SCF}_3 \text{ or } \text{C}(\text{CF}_3)_2\text{OH}$ (3 compounds)	38 ± 0.5 ( <i>MCF-7</i> ) $R^1 = \text{FcCH}_2, R^2 = \text{C}(\text{CF}_3)_2\text{OH}$ 4 cell lines	44
1.25/2a or 2b 	$R^1 = \text{Fc}$ $R^2 = \text{Me or Bn}; R^3 = \text{H, Cl, Br, Me}$ (24 compounds)	20.26 ( <i>MDA-MB-231</i> ) $R^1 = \text{FcCH}_2\text{OCH}_2, R^2 = \text{Me}, R^3 = \text{Br}$ 2 cell lines	45
1.26/2b 	$R =$ (A) or (B)	2.82 ± 0.14 ( <i>MDA-MB-231</i> ) $R = \text{A}$ 4 cell lines	46
1.27/2b 	$R = \text{CH}_2\text{Ph}$ (A) (B) or (C)	9.0 ± 0.03 ( <i>MCF-7</i> ) $R = \text{B}$ 3 cell lines	47



Table 1 (Contd.)

Entry/synthesis <sup>b</sup> structure and number of compounds examined	IC <sub>50</sub> or EC <sub>50</sub> [μM] (cell line) number of cancer cell lines studied	Ref.
1.28/2b  R = Ph (A) X = S or Se (6 compounds)	2.9 ± 0.25 (A549) R = B, X = Se 4 cell lines	48
1.29/2b <sup>c</sup>  (7 compounds, for details see Scheme 3)	5 ± 1 (A2780, DU-145) 3 cell lines	49–51
1.30/2c  R <sup>1</sup> , R <sup>2</sup> = H R <sup>1</sup> R <sup>2</sup> = (CH <sub>3</sub> ) <sub>2</sub> C-C(CH <sub>3</sub> ) <sub>2</sub> R <sup>3</sup> = <sup>18</sup> F or <sup>19</sup> F X = CH <sub>2</sub> or  (6 compounds)	20 ± 7 (MCF-7) R <sup>1</sup> , R <sup>2</sup> = Me <sub>2</sub> C-CMe <sub>2</sub> , R <sup>3</sup> = <sup>19</sup> F, X =  5 cell lines	52 and 53
1.31 <sup>g</sup> 	5.4 (HeLa) 4 cell lines	54

<sup>a</sup> IC<sub>50</sub> or EC<sub>50</sub> [μM] for the most active compound for the selected cell line is given. <sup>b</sup> See Scheme 1 for general click-chemistry synthetic approaches. <sup>c</sup> See text for details on the mechanism of action. <sup>d</sup> Synthesized by the post-click C–H arylation. <sup>e</sup> These compounds displayed also antimicrobial activity (R = C; MIC = 4.68 mg mL<sup>-1</sup>, *Micrococcus luteus*). <sup>f</sup> The corresponding ruthenocenes were also obtained and found to display comparable activity. <sup>g</sup> Synthesized using post-click amide coupling. Fc = ferrocenyl.

(entry 1.18; Scheme 2).<sup>39,40</sup> Interestingly, besides the 1,4-disubstitution pattern of the 1*H*-1,2,3-triazole scaffold, 1,5-isomers (compounds **1**) were also employed. It is worth noting that the 1,5-isomer (compound **1d**, IC<sub>50</sub> = 9.9 ± 0.5 μM) was less active than the corresponding 1,4-isomer (compound **2d**, IC<sub>50</sub> = 0.7 ± 0.1 μM). Taking into account the connectivity between ferrocene and 1*H*-1,2,3-triazole, three groups of derivatives could be classified: (a) compounds **1–3** with an *ortho*- or *para*-substituted chalcone linker, (b) derivatives **4–6** with a methylene linker, and (c) derivative **7** without any linker. Examination of all the derivatives in terms of their *in vitro* cytostatic effect toward hepatocellular carcinoma (*HepG2*) cells or colon cancer (*HT-29*) cells revealed high inhibitory activity of the chalcone-containing compounds **1–3** with IC<sub>50</sub> values ranging from 0.7 ± 0.1 μM (compound **1d**) to 14.3 ± 14.5 μM (compound **2b**) in the *HepG2* cell line, or 1.5 ± 0.2 μM (compound **1d**) to 6.6 ± 7.7 μM (compound **3d**) in the *HT-29* cell line.<sup>39</sup> It is worth mentioning that the observed inhibitory activity of compounds

**1–3** was much higher than that of their parent ferrocene-chalcone azides. This observation might suggest a considerable contribution of the cinchona alkaloid moiety to the inhibitory effect of hybrids **1–3**. Next, further examination of compounds **2a–d** addressed their activity against multidrug resistant (MDR) cancer cell lines of non-small cell lung carcinoma *NCI-H460/R*, colorectal carcinoma *DLD1-TxR* or glioblastoma *U87-TxR*.<sup>40</sup> Compounds **2c** and **2d** were the most interesting among the tested derivatives because they showed significantly higher cytotoxicity towards MDR glioblastoma *U87-TxR* cells (**2c**, IC<sub>50</sub> 3.13 ± 0.06 μM; **2d**, IC<sub>50</sub> 2.30 ± 0.02 μM) or colorectal carcinoma *DLD1-TxR* cells (**2d**, IC<sub>50</sub> 4.43 ± 0.06 μM) than towards the corresponding sensitive counterparts of the evaluated cancer cells. The anticancer activity of compound **2d** was postulated to be a consequence of its pro-oxidative effect, reflected by the extreme increase in the hydrogen peroxide and peroxy-nitrite anion concentrations in colorectal carcinoma *DLD1-TxR* cells or glioblastoma *U87-TxR* cells.





**Scheme 2** 1*H*-1,2,3-Triazole-tethered cinchona alkaloid-ferrocene hybrids (Table 1, entry 1.18).<sup>39,40</sup> Fc = ferrocenyl.



**Scheme 3** *N*-Alkylaminoferrocene-based prodrugs targeting the lysosomes of cancer cells (compound 8a<sup>49</sup>) or mitochondria of cancer cells (compounds 8b–g<sup>50,51</sup>). Table 1, entry 1.29.





Mokhir and co-workers developed a group of *N*-alkylaminoferrocene-based prodrugs **8** (entry 1.29; Scheme 3) targeting the lysosomes of cancer cells (compound **8a**<sup>49</sup>) or mitochondria of cancer cells (compounds **8b–g**<sup>50,51</sup>). Compound **8a** was toxic towards *BL-2* cells (IC<sub>50</sub> 27 ± 3 μM). Coumarin-induced ROS quenching was postulated to play a role in the moderate cytotoxicity of this compound. Accumulation of compound **8a** in cancer cell-specific lysosomes and its activation in these organelles was detected.<sup>49</sup> Among compounds **8b–e**, bearing a clinically approved drug carboplatin, conjugate **8b** was found to accumulate in the mitochondria of *A2780* cells more efficiently than the parent carboplatin.<sup>50</sup> This was reflected by the substantially higher anticancer effect of conjugate **8b** towards *A2780* cells than that of carboplatin at all incubation times (*e.g.* IC<sub>50</sub> at 96 h: 20 ± 1 vs >82 ± 7 μM, respectively). The synergistic effect of the platinum and the ferrocene components was postulated for compound **8b** owing to the fact that its activity was significantly higher than that of an equimolar mixture of reference compound **8c** and carboplatin. Compound **8f** exhibited higher efficiency of cellular uptake (*BL-2* cell line) than reference compound **8c**. Moreover, it exerted overall stronger effects on the cell viability in all studied cancer cell lines (*BL-2*, *A2780*, *DU-145*) than the reference compound **8c**, compound **8g**, or ferrocene, but it was less potent than an unspecific positive control (*i.e.* a mixture of FeCl<sub>3</sub> and 8-hydroxyquinoline).<sup>51</sup> Analogous to the reference compound **8c** and butyltriphenylphosphonium iodide, compound **8f** was found to kill the cancer cells mostly *via* necrosis and apoptosis with the former cell death phenotype being more prominent. All tested compounds were more active than ferrocene used as a control.

### 3 Conjugates with antibacterial and/or antifungal activity

Ferrocene-1*H*-1,2,3-triazole conjugates have been tested for antimicrobial activity in a limited number of studies (Table 2). In view of their structural features, molecules combining ferrocene and a scaffold with well-established antitubercular activity, such as isatin (entries 2.1 and 2.3) or isatin oxime (entry 2.7), are worth noting.

The mechanism of action of compounds summarized in Table 2 was not studied. Some conjugates were reported to show higher (entry 2.6) or comparable activity (entries 2.6 and 2.7) as the reference drugs (streptomycin sulphate for antibacterial activity or fluconazole for antifungal activity). The contribution of the ferrocene core to the antimicrobial activity of the conjugates was revealed by comparative assays employing a structurally resembling non-ferrocene counterpart (entry 2.7).<sup>60</sup> Moreover, the authors concluded that suitable substitution of the isatin oxime ring plays an important role in the observed activity. The same research group reported also several 3-ferrocenylidene-2-oxoindole conjugates with moderate antibacterial activity.<sup>62</sup> Weak, ultrasound-assisted antibac-

terial activity (*E. coli*) was also reported for a ferrocene-triazole-linked porphyrin.<sup>63</sup>

With the exception of a dendrimer (Table 1, entry 1.31), all examples presented here thus far belonged to the category of small molecules. A different approach was adopted by Lakouraj *et al.* who obtained a ferrocene-embedded polymer **11** containing azine and xanthone scaffolds as potential pharmacophores (Scheme 4).<sup>64</sup> A click-chemistry approach was used to assemble the target polymer **11** from monomers **9** and **10**. Polymer **11** showed antibacterial activity towards *E. coli*, *P. aeruginosa*, *K. pneumoniae*, *B. subtilis*, and *S. aureus* with a MIC concentration of 125 μg mL<sup>-1</sup> and MBC concentrations ranging from 250 to 500 μg mL<sup>-1</sup>. Additionally, at 100 μg mL<sup>-1</sup> polymer **11** showed a 20–40% decrease in the viability of *HeLa* cells, *MCF-7* cells, or *Saos* cells. Based on its unique antibacterial characteristics, potential industrial applications of polymer **11** were suggested, for instance, as a component of chemical coatings in medical devices used in hospitals.

### 4 Conjugates with antiprotozoa activity

Ferroquine completed the second phase of clinical trials with patients suffering from uncomplicated *P. falciparum* malaria.<sup>65</sup> Therefore, constant interest in potential ferrocene-antimalarial drugs bearing the 7-chloro-4-quinolinyl moiety has been observed (Table 3, entries 3.1, 3.2 and 3.3). Studies devoted to antiprotozoa activity (including antimalarial activity) of the isatin- or isatin derivative-bearing conjugates could be considered as a promising field (entries 3.4, 3.5, 3.6 and 3.7).

The study of a library of conjugates combining the 7-chloro-4-quinolinyl moiety and a ferrocene chalcone (in its ferrocene carboxaldehyde-originated variant, entries 3.1, 3.2, and 3.3) allowed the identification of the carbon chain as the most advantageous linker between these two pharmacophores (entry 3.1 vs. entries 3.2 and 3.3).<sup>41</sup> Although the most promising conjugates did not reach antiprotozoa activity of chloroquine or ferroquine, some of them showed IC<sub>50</sub> < 1 μM.

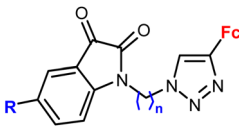
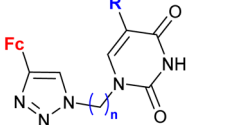
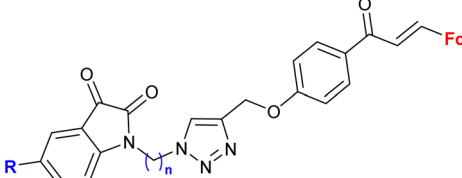
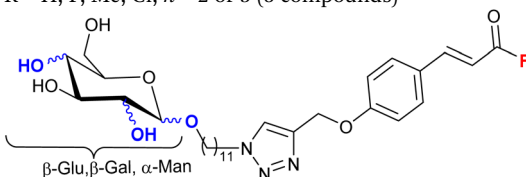
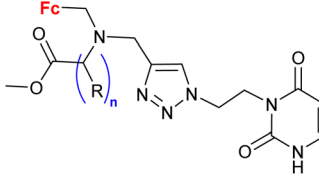
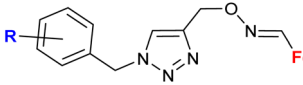
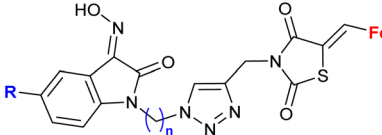
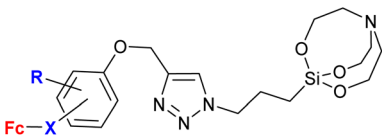
Evaluating several isatin-bearing conjugates as potential agents against *T. vaginalis* (entries 3.5, 3.6 and 3.7), Singh *et al.* found the isatin substitution pattern as the key factor determining the activity of the assayed conjugates (entry 3.7 vs. entries 3.5 and 3.6).<sup>67</sup> The conjugates were not active against normal human flora consisting of non-pathogenic strains: *Lactobacillus reuteri* (ATCC 23272), *Lactobacillus acidophilus* (ATCC 43560), and *Lactobacillus rhamnosus* (ATCC 53103). However, none of them was as active as the reference metronidazole.

A significantly different approach by Singh *et al.* resulted in ferrocene-chalcones linked through 1*H*-1,2,3-triazole to organosilatrane. These structurally unique compounds possessed strong activity against *G. lamblia* (entry 3.8). The same compounds were also tested against some bacterial and fungal strains, but showed only weak activity (see Table 2, entry 2.8).



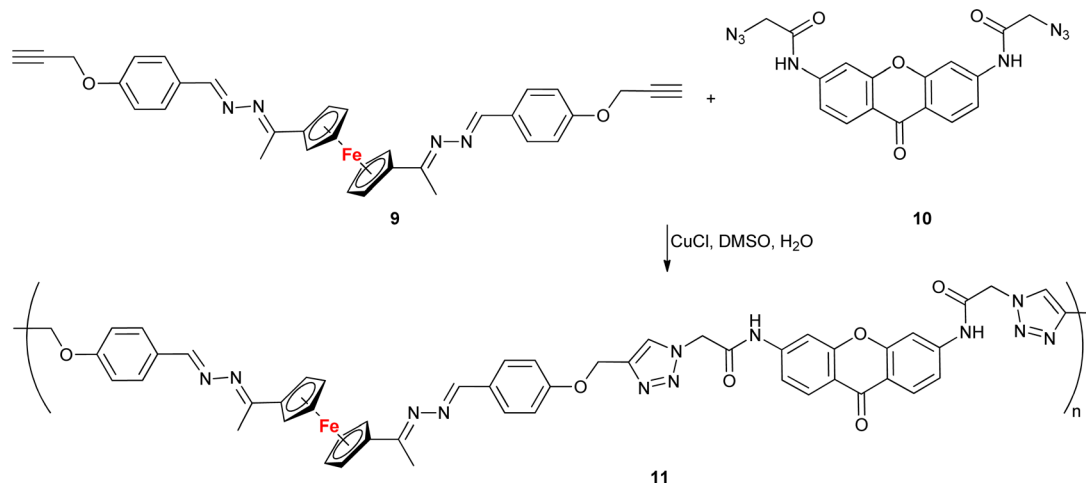


**Table 2** Ferrocene-1*H*-1,2,3-triazole conjugates with antibacterial and/or antifungal activity<sup>a</sup>

Entry/synthesis <sup>b</sup> structure and number of compounds examined	Activity (bacterial or fungal strain)	Ref.
2.1/2a  R = H, F, Me, Cl <i>n</i> = 2 or 3 (8 compounds)	MIC = 105–211 μM ( <i>M. tuberculosis mc</i> <sup>2</sup> 7000) R = Cl, <i>n</i> = 3	55
2.2/2a  R = H, Cl, Br <i>n</i> = 2–6, 8 (18 compounds)	MIC = 26.67 ± 1.67 μM ( <i>M. tuberculosis mc</i> <sup>2</sup> 6230) R = Br, <i>n</i> = 3 or 6	56
2.3/2b  R = H, F, Me, Cl, <i>n</i> = 2 or 3 (8 compounds)	MIC > 155 μM ( <i>M. tuberculosis mc</i> <sup>2</sup> 7000) R = Cl, <i>n</i> = 3	55
2.4/2b  R = H, F, Me, Cl, <i>n</i> = 2 or 3 (8 compounds)	Active <i>in vitro</i> as ampicillin against <i>E. coli</i> or <i>S. aureus</i> 2 bacterial strains 2 fungal strains	57
2.5/2b  R = H or ( <i>S</i> )-Me; <i>n</i> = 1–3 (4 compounds)	15 mm growth inhibition zone ( <i>C. guilliermondii</i> IBA 155) R = ( <i>S</i> )-Me, <i>n</i> = 1 15 bacterial strains 6 yeast strains	58
2.6/2b  R = H, 4-F, 4-Cl, 4-Br, 4-CF <sub>3</sub> , 4-OMe, 3-CF <sub>3</sub> , 3-Cl (8 compounds)	MIC = 7.81 μg mL <sup>-1</sup> ( <i>S. aureus</i> ) R = 4-F 4 bacterial strains 1 fungal strain	59
2.7/2b  R = Me, OMe, Cl, F, Br; <i>n</i> = 3 or 4 (10 compounds)	MIC = 4 μg mL <sup>-1</sup> ( <i>e.g. B. subtilis</i> , <i>M. smegmatis</i> , <i>E. coli</i> , or <i>C. albicans</i> ) <i>n</i> = 3: R = Me or OMe <i>n</i> = 4: R = Me or Cl, 8 bacterial strains 2 fungal strains	60
2.8/2b  R = H or OMe; X = -C(O)=CH- or -CH=C(O)- (6 compounds)	31.25 μM ( <i>C. albicans</i> ) R = OMe-4, X = (-CH=C(O)-)-3 7 fungal strains 6 bacterial strains	61

<sup>a</sup> Representative values of MIC for each class of compounds if given by the authors. <sup>b</sup> See Scheme 1 for general click-chemistry synthetic approaches. Fc = ferrocenyl.





**Scheme 4** Click-assembled polymer **11** composed of ferrocene, azine and xanthone scaffolds as potential pharmacophores.<sup>64</sup>

## 5 Conjugates with other types of activity

This section includes conjugates evaluated as inhibitors of cancer-associated enzymes (Table 4 entries 4.3 and 4.4) or HIV-1-associated enzymes (entry 4.5), and neuroprotective or anti-inflammatory agents (entry 4.6). Among these structurally diverse conjugates, a broad panel of benzenesulfonamides (entry 4.7) or oligopeptides (entry 4.5) are worth noting.

Salmon *et al.* showed the significant contribution of the ferrocenyl group to the activity of the benzenesulfonamide-bearing conjugates (Table 4, entry 4.7) towards selected carbonic anhydrases when compared to the corresponding ferrocene lacking counterparts, that is phenyl-containing compounds.<sup>77</sup> Moreover, several ruthenocene analogues were also studied to reveal higher or comparable activity of ruthenocene *vs.* ferrocene systems. The 1,5-disubstitution pattern of the 1*H*-1,2,3-triazole ring was identified as one of the factors determining high enzyme inhibitory activity. The benzene substitution pattern of the conjugates affected their enzyme inhibitory activity. However, water solubility and *in vitro* metabolic stability did not have an effect on their lipophilicity or *in vitro* permeability.

Peptide mimetic **12** (entry 4.5, Scheme 5) with nanomolar affinity for the HIV-1 surface protein gp120 and strong potency for inhibiting host cell infection was designed by the research group of Chaiken.<sup>79</sup> This compound was then used to identify the minimum-length active dual-antagonist sequence **13**<sup>80</sup> and a family of inhibitors of HIV-1 entry into host cells, including short-peptides **14–16** and cyclopeptides **17** and **18**.<sup>71–74</sup> The docking examination of the identified inhibitors suggested the crucial role of the ferrocene moiety in their binding to protein gp120.<sup>72</sup> The examined inhibitor–protein complexes were stable when their ferrocene moiety was buried in the protein site 2 hydrophobic cavity

by several hydrophobic interactions with the protein residues. Interestingly, the 1,5-disubstituted 1*H*-1,2,3-triazole analogue of peptide p1 was inactive. In the light of *in silico* recognized instability of the corresponding peptide–protein complex, these experimental findings confirmed the importance of the 1,4-disubstituted 1,2,3-triazole pattern to retain the ferrocene moiety inside the protein site 2 hydrophobic cavity. Cyclopeptides **17** and **18** greatly resisted *in vitro* proteolysis as demonstrated by their stability against trypsin and chymotrypsin.<sup>74</sup>

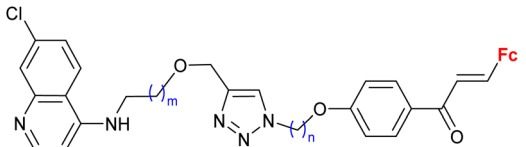
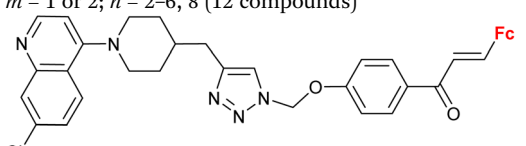
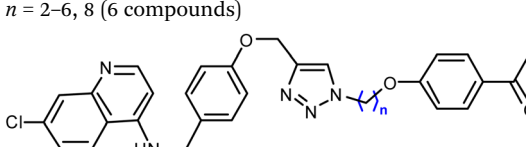
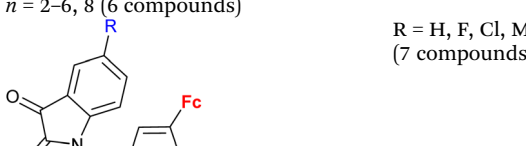
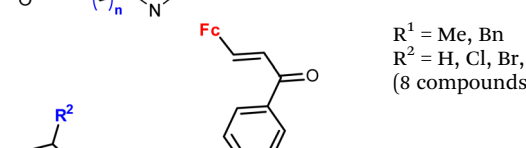
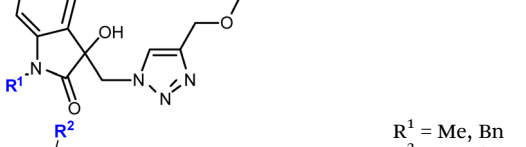
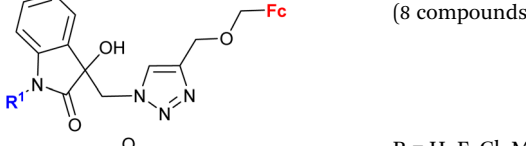
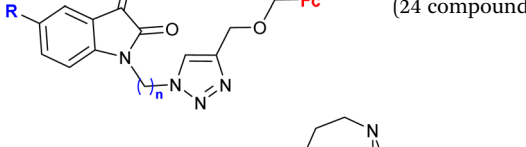
## 6 Challenges and outlook

The preparative versatility of the regioselective 1*H*-1,2,3-triazole-forming click-reaction can be considered as one of the factors stimulating the recent advances in the field of ferrocene-originating drug development. The undoubtedly broad synthetic scope of this approach has been employed to obtain a variety of new conjugates resulting from the attachment of ferrocene to a medically important molecule (*e.g.* isatin, a nucleobase, a carbohydrate, or an alkaloid framework), or by combining ferrocene (or a ferrocene-based privileged structure, such as ferrocene chalcones) with a structural unit(s) with well-documented pharmacophore activity (*e.g.* sulfonamide group or polyhydroxybenzene moiety). The latter strategy afforded a variety of structurally diverse *de novo* conjugates. The majority of new molecular entities discussed in this review have been evaluated for their anti-cancer potency. In general, the data summarized in this review suggest the advisability of comparative studies on structure–activity optimizations in terms of (a) the ferrocene-1*H*-1,2,3-triazole distance, (b) the construction of a ferrocene-1*H*-1,2,3-triazole linker (when present), and (c) the 1*H*-1,2,3-triazole ring orientation/substitution pattern.

The 1,5-disubstitution of the 1*H*-1,2,3-triazole ring could be considered as a worthwhile option since certain conjugates



**Table 3** Ferrocene-1*H*-1,2,3-triazole conjugates with antiprotozoa activity<sup>a</sup>

Entry/synthesis <sup>b</sup> structure and number of compounds examined	IC <sub>50</sub> (μM) ( <i>protozoa strain</i> )	Ref.
<b>3.1/1b</b>  <i>m</i> = 1 or 2; <i>n</i> = 2–6, 8 (12 compounds)	0.37 ± 0.03 μM ( <i>P. falciparum</i> W2) <i>m</i> = 2, <i>n</i> = 5	41
<b>3.2/1b</b>  <i>n</i> = 2–6, 8 (6 compounds)	2.55 ± 0.25 ( <i>P. falciparum</i> W2) <i>n</i> = 2	41
<b>3.3/1b</b>  <i>n</i> = 2–6, 8 (6 compounds)	1.16 ± 0.04 ( <i>P. falciparum</i> W2) <i>n</i> = 8	41
<b>3.4/2a</b>  <i>R</i> = H, F, Cl, Me <i>n</i> = 2, 3 (7 compounds)	3.76 ( <i>P. falciparum</i> 3D7) <i>R</i> = F, <i>n</i> = 3 2 protozoa strains	66
<b>3.5/2b</b>  <i>R</i> <sup>1</sup> = Me, Bn <i>R</i> <sup>2</sup> = H, Cl, Br, Me (8 compounds)	28.9 ( <i>T. vaginalis</i> ) <i>R</i> <sup>1</sup> = Bn, <i>R</i> <sup>2</sup> = Me	67
<b>3.6/2b</b>  <i>R</i> <sup>1</sup> = Me, Bn <i>R</i> <sup>2</sup> = H, Cl, Br, Me (8 compounds)	27.0 ( <i>T. vaginalis</i> ) <i>R</i> <sup>1</sup> = Bn, <i>R</i> <sup>2</sup> = Cl	67
<b>3.7/2b</b>  <i>R</i> = H, F, Cl, Me <i>n</i> = 2–6, 8 (24 compounds)	2.26 ( <i>T. vaginalis</i> ) <i>R</i> = Me, <i>n</i> = 5	68
<b>3.8/2b</b>  <i>R</i> = H or OMe; <i>X</i> = –C(O)=CH– or –CH=C(O)– (6 compounds)	0.57 ( <i>G. lamblia</i> ) <i>R</i> = H, <i>X</i> = –CH=C(O)– <i>ortho</i> isomer 2 protozoa strains	61

<sup>a</sup> Representative values of IC<sub>50</sub> (μM) for each class of compounds. <sup>b</sup> See Scheme 1 for general click-chemistry synthetic approaches. Fc = ferrocenyl.



Table 4 Ferrocene-1*H*-1,2,3-triazole conjugates with other biological effects<sup>a</sup>

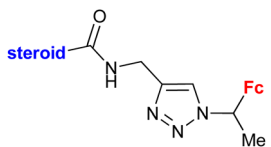
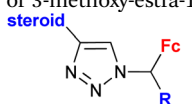
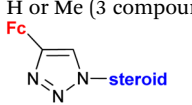
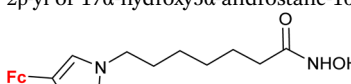
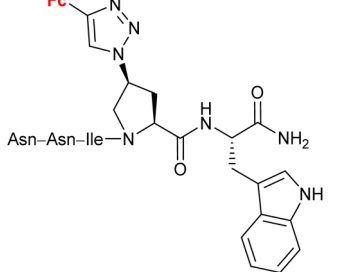
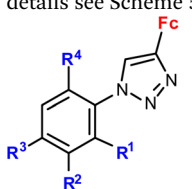
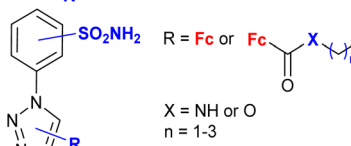
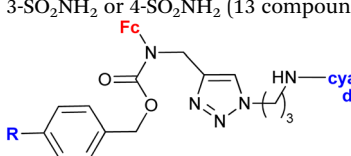
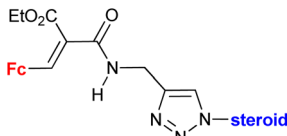
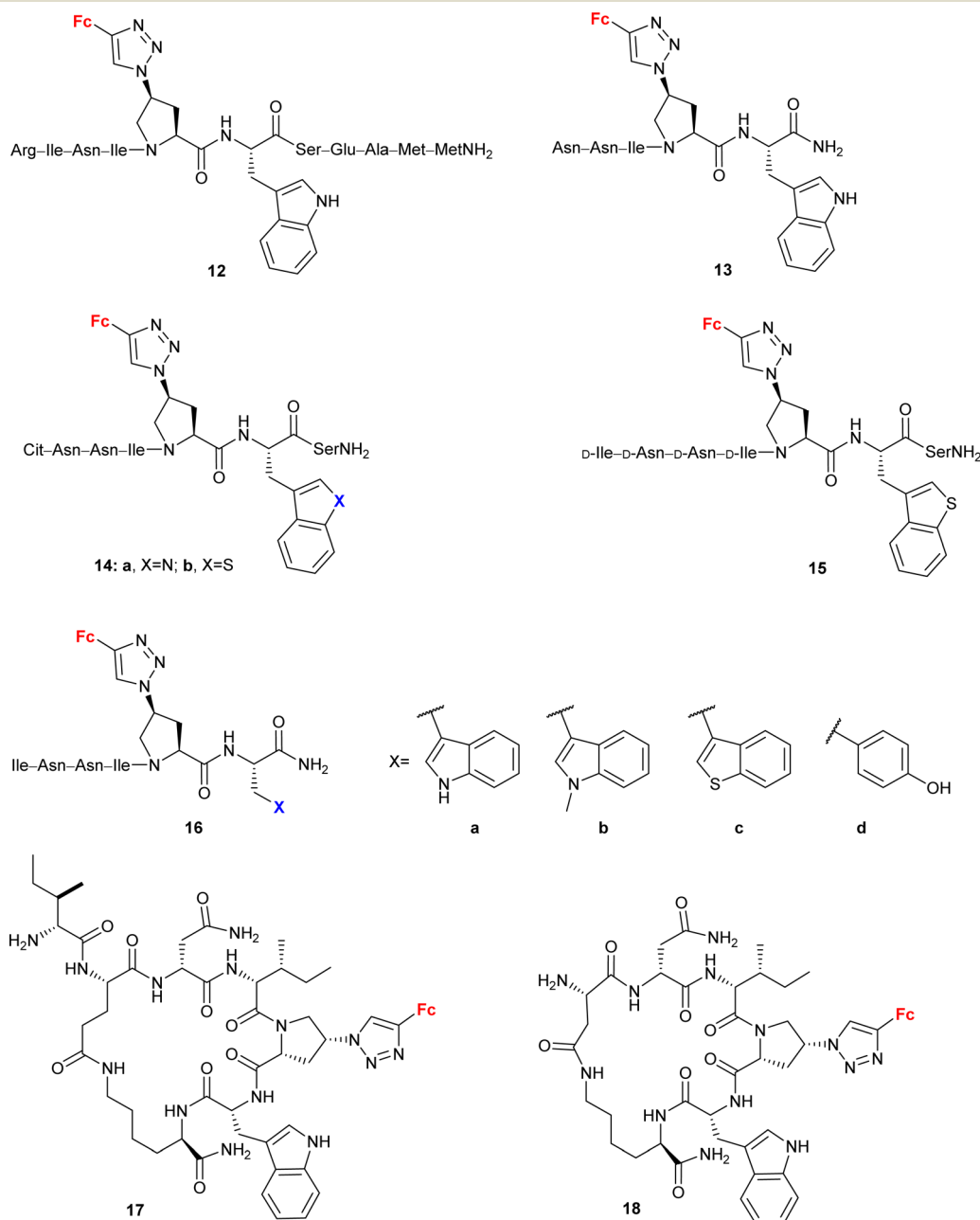
Entry/synthesis <sup>b</sup> structure and number of compounds examined	Effect/object of study	Ref.
<b>4.1/1a</b>  Steroid = 4-aza-5 $\alpha$ -androst-16-en-3-one-17-yl or 3-methoxy-estra-1,3,5(10),16-tetraene-17-yl	Inhibitory activity towards enzymes of the estrogen biosynthesis: the cytochrome P450-dependent aromatase, steroid sulfatase (STS), 17 $\beta$ -hydroxysteroid dehydrogenases type 1 (17 $\beta$ -HSD1) relative conversion = 65 $\pm$ 13% (17 $\beta$ -HSD1) steroid = 4-aza-5 $\alpha$ -androst-16-en-3-one-17-yl	69
<b>4.2/1b</b>  Steroid = estradiol-17 $\alpha$ -yl, 3,17 $\beta$ -dihydroxy-estra-1,3,5(10)-triene-17 $\alpha$ -yl, 17 $\beta$ -hydroxy-18a-homo-19-nor-androst-4-ene-3-one-17 $\alpha$ -yl R = H or Me (3 compounds)	Inhibitory activity towards enzymes of the estrogen biosynthesis: the cytochrome P450-dependent aromatase, steroid sulfatase (STS), 17 $\beta$ -hydroxysteroid dehydrogenases type 1 (17 $\beta$ -HSD1) IC <sub>50</sub> 0.0350 $\pm$ 0.0058 $\mu$ M (STS) steroid = 3,17 $\beta$ -dihydroxy-estra-1,3,5(10)-triene-17 $\alpha$ -yl R = Me	69
<b>4.3/2a</b>  Steroid = 3 $\alpha$ -hydroxy-5 $\alpha$ -androstane-17-one-2 $\beta$ -yl or 17 $\alpha$ -hydroxy-5 $\alpha$ -androstane-16 $\beta$ -yl	Inhibitory activity towards enzymes of the estrogen biosynthesis: the cytochrome P450-dependent aromatase, steroid sulfatase (STS), 17 $\beta$ -hydroxysteroid dehydrogenases type 1 (17 $\beta$ -HSD1) IC <sub>50</sub> 4.63 $\pm$ 1.51 $\mu$ M (STS) steroid = 3 $\alpha$ -hydroxy-5 $\alpha$ -androstane-17-one-2 $\beta$ -yl	69
<b>4.4/2a<sup>c</sup></b> 	Inhibition of histone deacetylase ( <i>HDAC1</i> , <i>HDAC2</i> , <i>HDAC3</i> or <i>HDAC6</i> ) IC <sub>50</sub> 0.0026 $\pm$ (0.0002) $\mu$ M ( <i>HDAC6</i> )	70
<b>4.5/2a<sup>c</sup></b>  Asn-Asn-Ile-N	Inhibitory activity towards protein gp120	71–74
<b>4.6/2a</b>  R <sup>1</sup> = H, NO <sub>2</sub> R <sup>2</sup> = H, Cl R <sup>3</sup> = H, F, Br R <sup>4</sup> = H or -C <sub>6</sub> H <sub>4</sub> -NO <sub>2</sub> -4 (5 compounds)	Low toxicity, non-inflammatory effect ( <i>BV-2</i> cells, <i>RMC</i> cells) and antioxidant activity ( <i>RMC</i> cells)	75 and 76
<b>4.7/2a or 2b<sup>c</sup></b>  X = NH or O n = 1–3 3-SO <sub>2</sub> NH <sub>2</sub> or 4-SO <sub>2</sub> NH <sub>2</sub> (13 compounds)	inhibition of carbonic anhydrase K <sub>i</sub> 3.2 nM $\pm$ 5–10% (CA II) R = 5-Fc, 3-SO <sub>2</sub> NH <sub>2</sub>	77
<b>4.8/2c</b> 	<i>In vitro</i> accumulation in A2780 cells, <i>in vivo</i> accumulation in tumours (AR42J or PC-3 tumour-bearing mice)	78



Table 4 (Contd.)

Entry/synthesis <sup>b</sup> structure and number of compounds examined	Effect/object of study	Ref.
4.9/2c  Steroid = 3 $\alpha$ -hydroxy-5 $\alpha$ -androstan-17-one-2 $\beta$ -yl, 3 $\alpha$ ,5 $\alpha$ -dihydroxyandrostan-17-one-6 $\beta$ -yl, 17 $\alpha$ -hydroxy-5 $\alpha$ -androstan-16 $\beta$ -yl	Inhibitory activity towards enzymes of the estrogen biosynthesis: the cytochrome P450-dependent aromatase, steroid sulfatase (STS), 17 $\beta$ -hydroxysteroid dehydrogenases type 1 (17 $\beta$ -HSD1) IC <sub>50</sub> 2.39 $\pm$ 1.10 $\mu$ M (STS) steroid = 17 $\alpha$ -hydroxy-5 $\alpha$ -androstan-16 $\beta$ -yl	69

<sup>a</sup> Representative examples of activity. <sup>b</sup> See Scheme 1 for general click-chemistry synthetic approaches. <sup>c</sup> See the text for details on the mechanism of action. Fc = ferrocenyl.



**Scheme 5** Peptide mimetics with nanomolar affinity for the HIV-1 surface protein gp120 and strong potency for inhibiting host cell infection (Table 4, entry 4.5).<sup>71–74</sup> Fc = ferrocenyl.



with this structural motif were reported to show greater biological potency than their 1,4-disubstituted counterparts. Interestingly, conjugates with more complex substitution patterns of the ferrocene scaffold than mono-substitution (including 1,1'-disubstitution or *ansa*-ferrocene, for instance) were infrequent. The activity of the *ansa*-ferrocene conjugate<sup>34</sup> suggested that structural modifications of the ferrocene core are an attractive route to new biologically active entities.

The effect of individual structural components of the conjugates on their biological activity was studied rather occasionally. When the ferrocene effect was examined, comparative *in vitro* SAR studies involved ferrocene-lacking counterparts of the target conjugates or their analogues with an aromatic substitute of ferrocene.<sup>60,69,77</sup> On the other hand, SAR studies evaluating a potential contribution of the 1*H*-1,2,3-triazole moiety employed the 1*H*-1,2,3-triazole-lacking counterpart<sup>43</sup> of the target conjugates or their amide or carbamide analogs.<sup>46,47,77</sup> In some cases, a comparison of the results seems rather difficult owing to the significant structural differences between the assayed conjugates (for instance, 1*H*-1,2,3-triazole-containing conjugates *vs.* chalcone-containing conjugates<sup>72</sup>).

Assays evaluating ferrocene-containing intermediates (azide<sup>34,39,58</sup> or alkyne,<sup>59</sup> or their precursor<sup>47,59</sup>) were also reported. Interestingly, Kocsis *et al.* gained a considerable increase in the cytostatic effect of the moderately active ferrocene-containing azide by linking it with cinchona alkaloid (Scheme 2, compound **1d**, IC<sub>50</sub> = 0.7 ± 0.1 μM *vs.* ferrocene-containing azide, IC<sub>50</sub> = 19.1 ± 1.3 μM).<sup>39</sup> Studies on conjugates with promising activity resulting from combining inactive ferrocene-originating 1*H*-1,2,3-triazole precursors with natural compounds (carbohydrates or nucleobases) are worth highlighting.<sup>34,47,58,59</sup> However, the ineffectiveness of ferrocene linking with an active conjugate precursor was also reported.<sup>37,55</sup>

Unfortunately, studies on the mode of action of these conjugates were not routine, that is, in many cases the biological results were limited to simple screening of the selected cell lines. Mechanistic investigations were pursued only for some classes of compounds displaying anticancer activity (Table 1). In most cases, the results suggested that the redox properties of the ferrocene core were important for the activity. In particular, Mokhir and co-workers identified *N*-alkylaminoferrocenium cations as active anticancer species.<sup>49–51</sup> This finding recalls the results of the first successful biological studies on ferrocenes that revealed the anticancer activity of some cationic derivatives.<sup>8,9</sup>

The redox properties of the ferrocene-triazole conjugates have been examined by cyclic voltammetry in several studies.<sup>31,33,37,38,43,47,54,59,60,75,76</sup> This technique has been employed mainly as a tool to characterize the new compounds rather than to find the relationship between the oxidation potential and biological activity. In two reports antioxidant activities were correlated with oxidation potentials.<sup>33,76</sup> However, in other studies such correlation was explicitly not observed<sup>31</sup> or not discussed.

Although infrequent, *in silico* studies of the mechanism of action of active conjugates brought added value to bioassay-

based screening. Molecular docking analyses revealed a considerable contribution of ferrocene and 1*H*-1,2,3-triazole cores to the biological activity of the conjugates. Chaiken *et al.* suggested hydrophobic interactions of both ferrocene and 1*H*-1,2,3-triazole with Env gp120 protein residues.<sup>72</sup> On the other hand, Khan *et al.* detected *H*-bonding interactions of 1*H*-1,2,3-triazole with cyclooxygenase-2 or cPLA2 protein residues.<sup>76</sup> Furthermore, *H*-bonding interactions between ferrocene and cPLA2 protein residues *via* the ferrocene iron atom were also suggested.

Having in mind an approximate character of such analysis at the current stage of these studies, we inspected the collected conjugates in terms of their potential to be selected as a hit compound in the early drug discovery process. The assayed series of compounds discussed in our review was rather small. For this reason, our selection was based on one-digit micromolar potency as a cut-off, in contrast to the 1 μM potency commonly employed in a real hit identification process.<sup>81</sup> In the light of the above criterion, within compounds reported to display anticancer activity, undoubtedly promising potency was exhibited by conjugates derived from quinoline (entries 1.2 and 1.19), deazapurine (entry 1.3), 4-quinolone (entry 1.7), uracil (entry 1.14), pyridine (entry 1.16), cinchona alkaloids (entry 1.18), carbohydrates (entries 1.23, 1.26, 1.27 and 1.28), phenylboronic acid (entry 1.29) and the polyamide dendrimer (entry 1.31). Interestingly, linking uracil with *ansa*-ferrocene (entry 1.11) or 5-iodouracil with ferrocene (entry 1.13) afforded conjugates endowed with promising potential exemplified by their *ca.* 10 μM potency. Fluorophenyl- (entry 2.6) and isatin oxime-bearing conjugates (entry 2.7) were noted as worth considering in the field of antibacterial drug development. On the other hand, ferrocene-conjugated derivatives of quinoline (entries 3.1–3.3), isatin (entries 3.4 and 3.7) and silatrane (entry 3.8) were found to possess antiprotozoa potency. Indisputably, our observation that quinoline- and isatin-bearing conjugates were reported to display a broad spectrum of biological activity (anticancer, antibacterial and antiprotozoa) might be an incentive to intensify research on ferrocene derivatives as potential drugs.

Taking into account that some contradictory data on the cytotoxicity of ferrocene have been reported,<sup>5,6,9,43,46,51,53</sup> it seems reasonable that ferrocene or its simple derivatives should be used as reference compounds in biological studies to facilitate the discovery of promising structural modifications.

## Abbreviations

Asn	Asparagine
D-Asn	D-Asparagine
AR42J	Rat pancreatic cancer cells
Arg	Arginine
A2780	Human ovarian adenocarcinoma cells
A549	Lung carcinoma cell line
BL-2	Burkitt lymphoma cells





BV-2	Murine microglial cell line
Cit	Citrulline
CFPAC-1	Pancreatic carcinoma cell line
DLD1-TxR	Multidrug resistant colorectal carcinoma cell line
DU-145	Human prostate carcinoma cells
Glu	Glutamic acid
HCC38	Breast carcinoma cell line
HeLa	Cervical carcinoma cell line
HepG2	Human hepatocyte carcinoma cell line
HL-60	Human promyelocytic leukemia cell line
HT-29	Colon cancer
Ile	Isoleucine
D-Ile	D-Isoleucine
K562	Chronic myelogenous leukemia cell line
Met	Methionine
MCF-7	Hormone-dependent breast cancer cell line
MDA-MB-231	Hormone-independent breast cancer cell line
MS	Melanoma cell line
NCI-H460/R	Multidrug resistant non-small cell lung carcinoma cell line
PC-3	Human prostate cancer cell line
Raji	Burkitt's lymphoma cell line
RD	Rhabdomyosarcoma cell line
RMC	Rat mesangial cells
ROS	Reactive oxygen species
SAR	Structure–activity relationship
Ser	Serine
Saos	Human osteosarcoma cell line
SW620	Colorectal carcinoma cell line
U87-TxR	Multidrug resistant glioblastoma cell line

## Conflicts of interest

There are no conflicts to declare.

## Acknowledgements

This work was financially supported by Warsaw University of Technology.

## References

- 1 T. J. Kealy and P. L. Pauson, *Nature*, 1951, **168**, 1039–1040.
- 2 P. Štěpnička, *Dalton Trans.*, 2022, **51**, 8085–8102.
- 3 I. M. Kolthoff and F. G. Thomas, *J. Phys. Chem.*, 1965, **69**, 3049–3058.
- 4 D. Osella, M. Ferrali, P. Zanello, F. Laschi, M. Fontani, C. Nervi and G. Cavigliolo, *Inorg. Chim. Acta*, 2000, **306**, 42–48.
- 5 I. H. Hall, A. E. Warren, C. C. Lee, M. D. Wasczak and L. G. Sneddon, *Anticancer Res.*, 1998, **18**, 951–962.
- 6 L. V. Snegur, Y. S. Nekrasov, N. S. Sergeeva, Z. V. Zhilina, V. V. Gumenyuk, Z. A. Starikova, A. A. Simenel, N. B. Morozova, I. K. Sviridova and V. N. Babin, *Appl. Organomet. Chem.*, 2008, **22**, 139–147.
- 7 V. J. Fiorina, R. J. Dubois and S. Brynes, *J. Med. Chem.*, 1978, **21**, 393–395.
- 8 P. Köpf-Maier, H. Köpf and E. W. Neuse, *Angew. Chem., Int. Ed. Engl.*, 1984, **23**, 456–457.
- 9 P. Köpf-Maier, H. Köpf-Maier and E. W. Neuse, *J. Cancer Res. Clin. Oncol.*, 1984, **108**, 336–340.
- 10 C. Biot, G. Glorian, L. A. Maciejewski, J. S. Brocard, O. Domarle, G. Blampain, P. Millet, A. J. Georges, H. Abessolo, D. Dive and J. Lebib, *J. Med. Chem.*, 1997, **40**, 3715–3718.
- 11 S. Top, J. Tang, A. Vessières, D. Carrez, C. Provot and G. Jaouen, *Chem. Commun.*, 1996, 955–956.
- 12 S. Top, A. Vessières, G. Leclercq, J. Quivy, J. Tang, J. Vaissermann, M. Huché and G. Jaouen, *Chem. – Eur. J.*, 2003, **9**, 5223–5236.
- 13 A. Vessières, S. Top, P. Pigeon, E. Hillard, L. Boubeker, D. Spera and G. Jaouen, *J. Med. Chem.*, 2005, **48**, 3937–3940.
- 14 D. Plazuk, A. Vessières, E. A. Hillard, O. Buriez, E. Labbé, P. Pigeon, M.-A. Plamont, C. Amatore, J. Zakrzewski and G. Jaouen, *J. Med. Chem.*, 2009, **52**, 4964–4967.
- 15 L. V. Popova, V. N. Babin, Y. A. Belousov, Y. S. Nekrasov, A. E. Snegireva, N. P. Borodina, G. M. Shaposhnikova, O. B. Bychenko, P. M. Raevskii, N. B. Morozova, A. I. Iiyina and K. G. Shitkov, *Appl. Organomet. Chem.*, 1993, **7**, 85–94.
- 16 The Nobel Prize in Chemistry 2022 was awarded to Carolyn R. Bertozzi, Morten Meldal and K. Barry Sharpless “for the development of click chemistry and bioorthogonal chemistry” during the reviewing of our contribution (5th October 2022).
- 17 E. Bonandi, M. S. Christodoulou, G. Fumagalli, D. Perdicchia, G. Rastelli and D. Passarella, *Drug Discovery Today*, 2017, **22**, 1572–1581.
- 18 K. Bozorov, J. Zhao and H. A. Aisa, *Bioorg. Med. Chem.*, 2019, **27**, 3511–3531.
- 19 D. Dheer, V. Singh and R. Shankar, *Bioorg. Chem.*, 2017, **71**, 30–54.
- 20 N. K. Verma, D. Mondal and S. Bera, *Curr. Org. Chem.*, 2020, **23**, 2305–2572.
- 21 A. Rani, G. Singh, A. Singh, U. Maqbool, G. Kaur and J. Singh, *RSC Adv.*, 2020, **10**, 5610–5635.
- 22 Carboxyamidotriazole (FDA UNII identifier, 6ST3ZF52WB; anticancer), cefatrizine (FDA UNII identifier, 8P4W949T8K; antibacterial), cefmatilen (FDA UNII identifier, T750UM24H8; antibacterial), rufinamide (FDA UNII identifier, WFW942PR79; anticonvulsant), tazobactam (FDA UNII identifier, SE10G96M8W; antibacterial), radezolid (FDA UNII identifier, 53PC6LO35W; antibacterial), mubritinib (FDA UNII identifier, V734AZP9BR; anticancer), solithromycin (FDA UNII identifier, 9U1ETH79CK; antibacterial), suvorexant (FDA UNII identifier, 081L192FO9; anti-insomnia), tradipitant (FDA UNII identifier, NY0COC51FI; anti-





- itchiness), flortanidazole F-18 (FDA UNII identifier, U6954O3II9; radioactive tumor hypoxia tracer). NCATS Inxight Drugs, <https://drugs.ncats.io/>, (accessed September 7, 2022).
- 23 D. K. Dalvie, A. S. Kalgutkar, S. C. Khojasteh-Bakht, R. S. Obach and J. P. O'Donnell, *Chem. Res. Toxicol.*, 2002, **15**, 269–299.
  - 24 V. Ganesh, V. S. Sudhir, T. Kundu and S. Chandrasekaran, *Chem. – Asian J.*, 2011, **6**, 2670–2694.
  - 25 G. Jaouen, A. Vessières and S. Top, *Chem. Soc. Rev.*, 2015, **44**, 8802–8817.
  - 26 K. Kowalski, *Coord. Chem. Rev.*, 2016, **317**, 132–156.
  - 27 M. Patra and G. Gasser, *Nat. Rev. Chem.*, 2017, **1**, e0066.
  - 28 R. Wang, H. Chen, W. Yan, M. Zheng, T. Zhang and Y. Zhang, *Eur. J. Med. Chem.*, 2020, **190**, e112109.
  - 29 V. Raičević, N. Radulović and M. Sakač, *Eur. J. Inorg. Chem.*, 2022, e202100951.
  - 30 D. R. van Staveren and N. Metzler-Nolte, *Chem. Rev.*, 2004, **104**, 5931–5986.
  - 31 D. Plažuk, B. Rychlik, A. Błaż and S. Domagała, *J. Organomet. Chem.*, 2012, **715**, 102–112.
  - 32 S. Maračić, J. Lapić, S. Djaković, T. Opačak-Bernardi, L. Glavaš-Obrovac, V. Vrček and S. Raić-Malić, *Appl. Organomet. Chem.*, 2019, **33**, e4628.
  - 33 V. Rep, M. Piškori, H. Šimek, P. Mišetić, P. Grbčić, J. Padovan, V. Gabelica Marković, D. Jadreško, K. Pavelić, S. Kraljević Pavelić and S. Raić-Malić, *Molecules*, 2020, **25**, e1570.
  - 34 M. Mazur, M. Mrozowicz, W. Buchowicz, M. Koszytkowska-Stawińska, R. Kamiński, Z. Ochal, P. Wińska and M. Bretner, *Dalton Trans.*, 2020, **49**, 11504–11511.
  - 35 S. Djaković, L. Glavaš-Obrovac, J. Lapić, S. Maračić, J. Kirchofer, M. Knežević, M. Jukić and S. Raić-Malić, *Appl. Organomet. Chem.*, 2021, **35**, e6052.
  - 36 L. V. Anikina, D. A. Shemyakina, L. V. Pavlogradskaya, A. N. Nedugov and V. A. Glushkov, *Russ. J. Org. Chem.*, 2014, **50**, 1180–1183.
  - 37 S. B. Deepthi, R. Trivedi, L. Giribabu, P. Sujitha and C. G. Kumar, *Inorg. Chim. Acta*, 2014, **416**, 164–170.
  - 38 S. Jakopec, N. Pantalon Juraj, A. Brozovic, D. Jadreško, B. Perić, S. I. Kirin and S. Raić-Malić, *Appl. Organomet. Chem.*, 2022, **36**, e6575.
  - 39 L. Kocsis, I. Szabó, S. Bősze, T. Jernei, F. Hudecz and A. Csámpai, *Bioorg. Med. Chem. Lett.*, 2016, **26**, 946–949.
  - 40 A. Podolski-Renić, S. Bősze, J. Dinić, L. Kocsis, F. Hudecz, A. Csámpai and M. Pešić, *Metallomics*, 2017, **9**, 1132–1141.
  - 41 A. Singh, J. Gut, P. J. Rosenthal and V. Kumar, *Eur. J. Med. Chem.*, 2017, **125**, 269–277.
  - 42 V. A. Glushkov, D. A. Shemyakina, N. K. Zhukova, L. V. Pavlogradskaya, M. V. Dmitriev, D. V. Eroshenko, A. R. Galeev and I. G. Mokrushin, *Russ. J. Org. Chem.*, 2019, **55**, 1690–1697.
  - 43 R. Trivedi, S. B. Deepthi, L. Giribabu, B. Sridhar, P. Sujitha, C. G. Kumar and K. V. S. Ramakrishna, *Eur. J. Inorg. Chem.*, 2012, 2267–2277.
  - 44 M. Maschke, M. Lieb and N. Metzler-Nolte, *Eur. J. Inorg. Chem.*, 2012, 5953–5959.
  - 45 A. Singh, S. T. Saha, S. Perumal, M. Kaur and V. Kumar, *ACS Omega*, 2018, **3**, 1263–1268.
  - 46 S. B. Deepthi, R. Trivedi, L. Giribabu, P. Sujitha and C. G. Kumar, *Dalton Trans.*, 2013, **42**, 1180–1190.
  - 47 S. B. Deepthi, R. Trivedi, L. Giribabu, P. Sujitha, C. G. Kumar and B. Sridhar, *New J. Chem.*, 2014, **38**, 227–236.
  - 48 S. Panaka, R. Trivedi, K. Jaipal, L. Giribabu, P. Sujitha, C. G. Kumar and B. Sridhar, *J. Organomet. Chem.*, 2016, **813**, 125–130.
  - 49 S. Daum, M. S. V. Reshetnikov, M. Sisa, T. Dumych, M. D. Lootsik, R. Bilyy, E. Bila, C. Janko, C. Alexiou, M. Herrmann, L. Sellner and A. Mokhir, *Angew. Chem., Int. Ed.*, 2017, **56**, 15545–15549.
  - 50 V. Reshetnikov, S. Daum, C. Janko, W. Karawacka, R. Tietze, C. Alexiou, S. Paryzhak, T. Dumych, R. Bilyy, P. Tripal, B. Schmid, R. Palmisano and A. Mokhir, *Angew. Chem., Int. Ed.*, 2018, **57**, 11943–11946.
  - 51 V. Reshetnikov, H. G. Özkan, S. Daum, C. Janko, C. Alexiou, C. Sauer, M. R. Heinrich and A. Mokhir, *Molecules*, 2020, **25**, e2545.
  - 52 J. Toms, V. Reshetnikov, S. Maschauer, A. Mokhir and O. Prante, *J. Labelled Compd. Radiopharm.*, 2018, **61**, 1081–1088.
  - 53 S. Daum, J. Toms, V. Reshetnikov, H. G. Özkan, F. Hampel, S. Maschauer, A. Hakimoun, F. Beierlein, L. Sellner, M. Schmitt, O. Prante and A. Mokhir, *Bioconjugate Chem.*, 2019, **30**, 1077–1086.
  - 54 D. L. Bertuzzi, C. B. Braga, G. Perli and C. Ornelas, *Eur. J. Inorg. Chem.*, 2022, e202101084.
  - 55 K. Kumar, S. Carrère-Kremer, L. Kremer, Y. Guéardel, C. Biot and V. Kumar, *Organometallics*, 2013, **32**, 5713–5719.
  - 56 A. Singh, C. Biot, A. Viljoen, C. Dupont, L. Kremer, K. Kumar and V. Kumar, *Chem. Biol. Drug Des.*, 2017, **89**, 856–861.
  - 57 M. R. E. Aly, I. H. El Azab and A. A. Gobouri, *Monatsh. Chem. Verw. Teile Anderer Wiss. Chem. Mon.*, 2018, **149**, 505–517.
  - 58 M. Daniluk, W. Buchowicz, M. Koszytkowska-Stawińska, K. Jarzabek, K. N. Jarzemska, R. Kamiński, M. Piszcz, A. E. Laudy and S. Tyski, *ChemistrySelect*, 2019, **4**, 11130–11135.
  - 59 Y. Swetha, E. R. Reddy, J. R. Kumar, R. Trivedi, L. Giribabu, B. Sridhar, B. Rathod and R. S. Prakasham, *New J. Chem.*, 2019, **43**, 8341–8351.
  - 60 S. Yagnam, R. Trivedi, S. Krishna, L. Giribabu, G. Praveena and R. S. Prakasham, *J. Organomet. Chem.*, 2021, **937**, e121716.
  - 61 G. Singh, A. Arora, P. Kalra, I. K. Maurya, C. E. Ruizc, M. A. Estebanc, S. Sinha, K. Goyal and R. Sehgal, *Bioorg. Med. Chem.*, 2019, **27**, 188–195.
  - 62 S. Yagnam, E. Rami Reddy, R. Trivedi, N. V. Krishna, L. Giribabu, B. Rathod, R. S. Prakasham and B. Sridhar, *Appl. Organomet. Chem.*, 2019, **33**, e4817.
  - 63 E. Yu. Rogatkina, A. N. Rodionov, S. E. Mazina and A. A. Simenel, *J. Porphyrins Phthalocyanines*, 2021, **25**, 31–36.



- 64 M. M. Lakouraj, V. Hasantabar, H. Tashakkorian and M. Golpour, *Polym. Adv. Technol.*, 2018, **29**, 2784–2796.
- 65 Sanofi, A Randomized, Open Label, Parallel-group, Single Dose Regimen, Phase 2a Study, to Investigate the Clinical and Parasitocidal Activity and the Pharmacokinetics of 3 Dose Levels of Artefenomel (OZ439) Given in Combination With Ferroquine (FQ) and FQ Alone, in African Patients With Uncomplicated Plasmodium Falciparum Malaria, [clinicaltrials.gov](https://clinicaltrials.gov), 2022.
- 66 K. Kumar, B. Pradines, M. Madamet, R. Amalvict, N. Benoit and V. Kumar, *Eur. J. Med. Chem.*, 2014, **87**, 801–804.
- 67 A. Singh, D. Zhang, C. C. Tam, L. W. Cheng, K. M. Land and V. Kumar, *J. Organomet. Chem.*, 2019, **896**, 1–4.
- 68 A. Singh, G. Fong, J. Liu, Y.-H. Wu, K. Chang, W. Park, J. Kim, C. Tam, L. W. Cheng, K. M. Land and V. Kumar, *ACS Omega*, 2018, **3**, 5808–5813.
- 69 B. E. Herman, J. Gardi, J. Julesz, C. Tömböly, E. Szánti-Pintér, K. Fehér, R. Skoda-Földes and M. Szécsi, *Biol. Futura*, 2020, **71**, 249–264.
- 70 J. Spencer, J. Amin, R. Boddiboyena, G. Packham, B. E. Cavell, S. S. Syed Alwi, R. M. Paranal, T. D. Heightman, M. Wang, B. Marsden, P. Coxhead, M. Guille, G. J. Tizzard, S. J. Coles and J. E. Bradner, *MedChemComm*, 2012, **3**, 61–64.
- 71 K. Kamanna, R. Aneja, C. Duffy, P. Kubinski, D. Rodrigo Moreira, L. D. Bailey, K. McFadden, A. Schön, A. Holmes, F. Tuzer, M. Contarino, E. Freire and I. M. Chaiken, *ChemMedChem*, 2013, **8**, 322–328.
- 72 R. Aneja, A. A. Rashad, H. Li, R. V. Kalyana Sundaram, C. Duffy, L. D. Bailey and I. Chaiken, *J. Med. Chem.*, 2015, **58**, 3843–3858.
- 73 A. A. Rashad, K. Acharya, A. Haftl, R. Aneja, A. Dick, A. P. Holmes and I. Chaiken, *Org. Biomol. Chem.*, 2017, **15**, 7770–7782.
- 74 A. A. Rashad, R. V. Kalyana Sundaram, R. Aneja, C. Duffy and I. Chaiken, *J. Med. Chem.*, 2015, **58**, 7603–7608.
- 75 A. Haque, M.-F. Hsieh, S. I. Hassan, Md. S. Haque Faizi, A. Saha, N. Dege, J. A. Rather and M. S. Khan, *J. Mol. Struct.*, 2017, **1146**, 536–545.
- 76 C.-Y. Cheng, A. Haque, M.-F. Hsieh, S. Imran Hassan, M. S. H. Faizi, N. Dege and M. S. Khan, *Int. J. Mol. Sci.*, 2020, **21**, e3823.
- 77 A. J. Salmon, M. L. Williams, Q. K. Wu, J. Morizzi, D. Gregg, S. A. Charman, D. Vullo, C. T. Supuran and S.-A. Poulsen, *J. Med. Chem.*, 2012, **55**, 5506–5517.
- 78 H. Gizem Özkan, J. Toms, S. Maschauer, O. Prante and A. Mokhir, *Eur. J. Inorg. Chem.*, 2021, 5096–5102.
- 79 H. Gopi, S. Cocklin, V. Pirrone, K. McFadden, F. Tuzer, I. Zentner, S. Ajith, S. Baxter, N. Jawanda, F. C. Krebs and I. M. Chaiken, *J. Mol. Recognit.*, 2009, **22**, 169–174.
- 80 M. Umashankara, K. McFadden, I. Zentner, A. Schön, S. Rajagopal, F. Tuzer, S. A. Kuriakose, M. Contarino, J. LaLonde, E. Freire and I. Chaiken, *ChemMedChem*, 2010, **5**, 1871–1879.
- 81 M. P. Gleeson, A. Hersey, D. Montanari and J. Overington, *Nat. Rev. Drug Discovery*, 2011, **10**, 197–208.

